



CrossMark
 click for updates

Cite this: *RSC Adv.*, 2017, 7, 4102

Immobilising a cobalt cubane catalyst on a dye-sensitised TiO₂ photoanode *via* electrochemical polymerisation for light-driven water oxidation†

Jialing Li,^a Yi Jiang,^{*ab} Qian Zhang,^a Xiaochen Zhao,^c Na Li,^{ad} Haili Tong,^a Xiaoxuan Yang^a and Lixin Xia^{*a}

A simple and effective method to prepare photocatalytically active electrodes for water oxidation is described in this paper. The precious-metal-free catalyst, Co₄O₄(O₂CMe)₄(4-vinylpy)₄ (py = pyridine) was electrochemically polymerised on a RuP-sensitised TiO₂ (RuP = [Ru(bpy)₂(4,4'-(PO₃H₂)₂bpy₂)]Cl₂) and on a TiO₂ surface codecorated with vinyl phosphate (Vpa) and RuP for applications in molecular photoelectrochemical (PEC) devices. With a Vpa chain as the anchoring group, the photoanode poly-Co₄O₄+Vpa/RuP/TiO₂ demonstrated a significantly higher PEC performance compared to poly-Co₄O₄/RuP/TiO₂. The introduction of a Vpa chain allows better immobilisation of catalyst and enhances the electron transport between the photosensitiser and the catalyst. A photocurrent density of ~100 μA cm⁻² was achieved in a Na₂SO₄ solution at pH 7.0 under a 0.4 V external bias, with a faradaic efficiency of 76% for oxygen production.

Received 10th October 2016
 Accepted 2nd November 2016

DOI: 10.1039/c6ra24989b

www.rsc.org/advances

Introduction

As the global demand for energy continually increases, the reduction in energy resources has become increasingly concerning. The development of sustainable and environmentally friendly energy resources is highly desirable. The utilisation of solar energy is believed to be one of the most promising ways in which to address this problem. Many schemes that utilise solar energy use photoelectrochemical (PEC) cells, the development of which is becoming popular in the field of solar energy conversion.^{1–8} In the PEC system, the overall process consists of two half-reactions: water oxidation to generate oxygen and proton reduction to produce hydrogen. The water oxidation half-reaction occurring in the photoanode is a four-proton and four-electron process requiring a high energy barrier and is considered as the limiting step in the PEC process.

Inspired by nature, scientists have investigated developing different types of metal complexes to be used as water oxidation catalysts.⁹ The most widely studied water oxidation catalysts are dependent on expensive transition metals, such as Ru and

Ir.^{10–15} The development of viable molecular catalysts based on low cost and earth-abundant elements have attracted great attention. Among the molecular catalysts, Co₄O₄(O₂CMe)₄(py)₄ (py = pyridine derivatives), are of particular interest because of their cubical core that mimics the oxygen-evolving complex (OEC) of PSII.^{16–18} Dismukes *et al.*¹⁶ reported photocatalytic activity for water oxidation in a three component system, a homogeneous aqueous solution consisting of a catalyst, a photosensitiser, and an electronic sacrificial acceptor. However, the existence of the electronic sacrificial acceptor (necessary in this homogeneous system) is not beneficial for practical application. In practical design, the immobilisation of a water oxidation catalyst onto the photoelectrode for construction of a PEC cell appears to be a promising approach. A number of strategies to integrate molecular chromophores and catalysts on metal oxide film have been explored for preparing dye-sensitized photoanodes, including carboxylate- or phosphonate-surface binding,^{19–21} preformed chromophore-catalyst assemblies.²² Self-assemblies such as “layer by layer”^{23,24} and others. However, most of the dye-sensitized photoanodes are based on Ru catalysts. To date only one cobalt cubane decorated photoanode has been reported in which a PEC photoanode is made from combining the cobalt cubane catalyst with Fe₂O₃.²⁵

Recently, Meyer reported the reductive electro-polymerisation of a vinyl-functionalised Ru catalyst on a TiO₂ surface which had been previously derivatised with a vinyl- and phosphonate-functionalised chromophore to produce a cross-linked film for PEC water oxidation.^{26,27} Sun reported an electro-oligomerisation of a Ru catalyst on a dye-sensitized TiO₂

^aCollege of Chemistry, Liaoning University, Shenyang 110036, Liaoning, China. E-mail: jiangyi@lnu.edu.cn; lixinxia@lnu.edu.cn

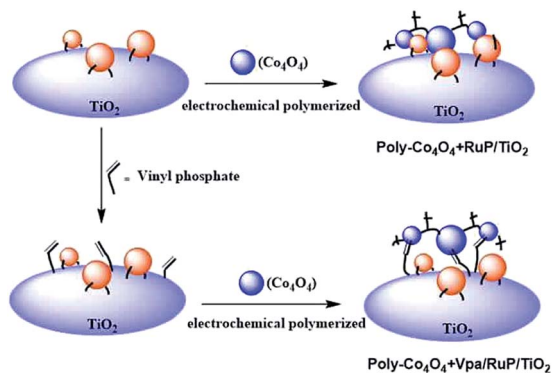
^bState Key Laboratory of Fine Chemicals, Dalian University of Technology, Dalian 116024, China

^cState Key Laboratory of Catalysis, Dalian Institute of Chemical Physics, Chinese Academy of Sciences, Dalian 116023, Liaoning, China

^dDepartment of Chemical Engineering, Yingkou Institute of Technology, Yingkou 115000, Liaoning, China

† Electronic supplementary information (ESI) available. See DOI: 10.1039/c6ra24989b





Scheme 1 Two types of photoanodes.

electrode and a Fe_2O_3 electrode.²⁸ This report describes two types of photoanodes produced by immobilising a vinyl-modified cobalt cubane water oxidation catalyst $\text{Co}_4\text{O}_4(\text{O}_2\text{-CMe})_4(4\text{-vinylpy})_4$ (Co_4O_4) onto a dye-sensitised RuP/TiO₂ electrode (RuP = $[\text{Ru}(\text{bpy})_2(4,4'-(\text{PO}_3\text{H}_2)_2\text{bpy}_2)]\text{Cl}_2$) *via* electrochemically polymerisation (Scheme 1). The PEC properties of the prepared photoanodes are described in this report.

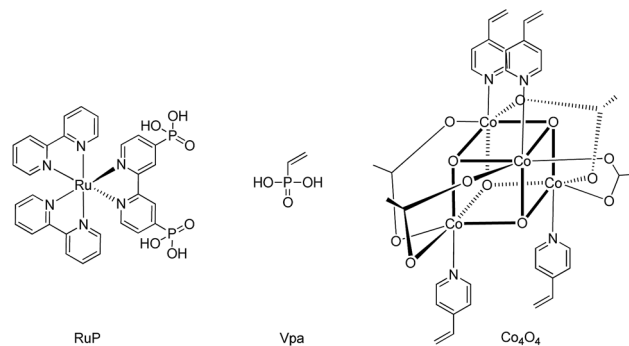
Results and discussion

¹H-NMR and MS data (Fig. S1[†]) confirmed a vinyl modified cubane cobalt was obtained, as the structure shown in Scheme 2. The Scanning Electron Microscopy (SEM) microstructures of TiO₂, RuP/TiO₂, poly- Co_4O_4 +RuP/TiO₂ load on the glass are shown in Fig. S2,[†] respectively. In Fig. S2A,[†] the TiO₂ photoanode shows a loose aggregation with the inter-particle pores which is to the benefit of the adsorption of the photosensitiser. In Fig. S2C,[†] a film layer can be shown, indicating of the polymerisation of the catalyst on the surface of the photoanode.

Electrochemical and photoelectrochemical measurements

The working electrodes was subjected to electrochemical tests. Cyclic voltammeters (CVs) of RuP/TiO₂ (red line), poly- Co_4O_4 +RuP/TiO₂ (blue line) and the bare TiO₂/FTO (black line) are shown in the Fig. 1. A reversible peak observed at $E_{1/2} = 1.31$ V (*vs.* NHE) (red line) is assigned to the redox couple of Ru^{II}/Ru^{III} for RuP. In comparison, the peak of poly- Co_4O_4 +RuP/TiO₂ (blue line) at $E_{1/2} = 1.0$ V (*vs.* NHE) is assigned to oxidation peak of Co^{III}/Co^{IV} for Co_4O_4 , followed by a steep oxidation peak current of water which is catalytically oxidized at a potential greater than 1.2 V. The results indicate that the poly- Co_4O_4 +RuP/TiO₂ electrode possesses water oxidation activity and the oxidized RuP can take electrons from poly- Co_4O_4 to realize water oxidation thermodynamically.

In order to measure the photoelectric property of the photoanode, a three-electrode PEC device consisting of poly- Co_4O_4 +RuP/TiO₂ as a photoanode, Ag/AgCl as a reference electrode, and Pt wire as a cathode was illuminated with visible light (>400 nm, 100 mW cm^{-2}) (red line) in a 0.1 M Na_2SO_4 solution as shown in Fig. 2. Applying different external conditions at below 0.8 V (*vs.* NHE), no obvious increase in photocurrent

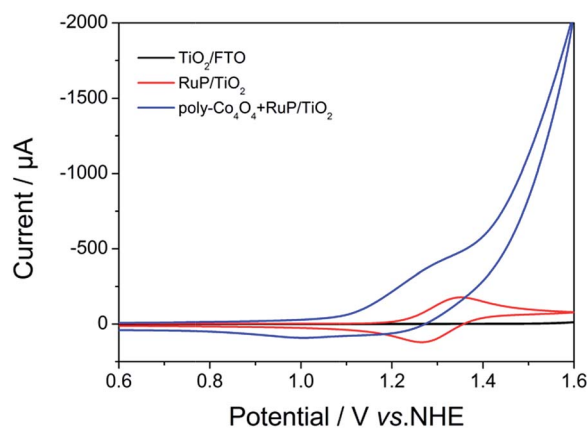


Scheme 2 Chemical structures of complexes.

density was observed with the increase of the potentials. It was observed that the current density of poly- Co_4O_4 +RuP/TiO₂ under light illumination was significantly higher than that without light illumination, and photolysis of water in the initial potential of 1.2 V (*vs.* NHE). This suggests that the photoanode consisting of molecular photosensitiser and catalyst has a good catalytic activity for light-driven water splitting.

To further improve the performance of such PEC device, we introduce a new type of photoanode by immobilizing $\text{Co}_4\text{O}_4(\text{O}_2\text{-CMe})_4(4\text{-vinylpy})_4$ on a TiO₂ surface codecorated with vinyl phosphate(Vpa) and RuP *via* electrochemically polymerisation. For preparation of the Co_4O_4 +Vpa/RuP/TiO₂ photoanode, the RuP/TiO₂ photoanode was first immersed in a methanol solution of Vpa, and then complex Co_4O_4 was electropolymerised on Vpa/RuP/TiO₂ films for 400 s. The UV-vis absorption spectra of the Vpa/RuP/TiO₂, poly- Co_4O_4 +Vpa/TiO₂, poly- Co_4O_4 +Vpa/RuP/TiO₂ were shown in Fig. S3,[†] respectively.

A series of electrochemical measurements were conducted for to investigate the PEC properties of the new type of photoanode. The CV measurements were applied in a 0.1 M Na_2SO_4 solution at pH 7.0 and the CV curves of Vpa/RuP/TiO₂ (red line), poly- Co_4O_4 +Vpa/RuP/TiO₂ (blue line) was shown in Fig. 3A. CV curves of RuP/TiO₂ (black line) and Vpa/RuP/TiO₂ (red line) in Fig. S4[†] showed that the Vpa did not significantly alter the redox potential of RuP (Fig. 3B). The poly- Co_4O_4 +Vpa/RuP/TiO₂

Fig. 1 CV curves of poly- Co_4O_4 +RuP/TiO₂ (blue line), RuP/TiO₂ (red line) and TiO₂/FTO (black line) in pH 7.0 Na_2SO_4 electrolyte (0.1 M).

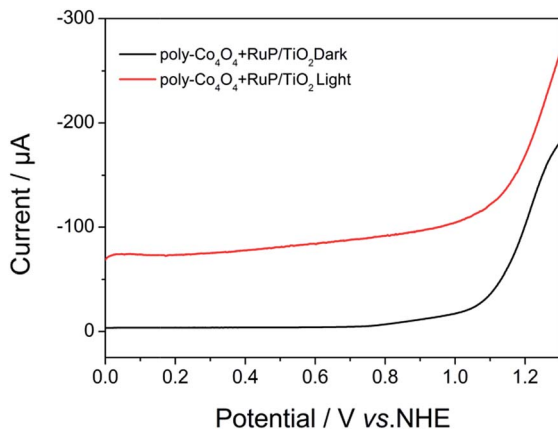


Fig. 2 Linear Sweep Voltammetry (LSV) of poly- $\text{Co}_4\text{O}_4+\text{RuP}/\text{TiO}_2$ carried out under illumination with a xenon lamp source coupled to a 400 nm long-pass filter (100 mW cm^{-2}) (red line) and non-light (black line).

exhibited a larger peak at an $E_{1/2}$ of 1.0 V (*vs.* NHE) for the $\text{Co}^{\text{III}}/\text{Co}^{\text{IV}}$ redox couple of catalyst (red line) compared to poly- $\text{Co}_4\text{O}_4/\text{RuP}/\text{TiO}_2$ (black line), indication of that the introduction of the Vpa chain increased the amount of the catalyst. In order to measure the amount of the photocatalyst and photosensitiser on the surface of the modified electrode, Differential Pulse Voltammograms (DPVs) tests were conducted in anhydrous acetonitrile solution (Fig. S5†). Comparing the areas of the redox peak of the catalyst ($\text{Co}^{\text{III}}/\text{Co}^{\text{IV}}$) at 1.0 V (*vs.* NHE) and the areas of the redox peak of the photosensitiser ($\text{Ru}^{\text{II}}/\text{Ru}^{\text{III}}$) at 1.5 V (*vs.* NHE), the ratio of photosensitiser and catalyst on the TiO_2 surface was obtained. The amount of the catalyst on poly- $\text{Co}_4\text{O}_4+\text{Vpa}/\text{RuP}/\text{TiO}_2$ is calculated to $1.0 \times 10^{-9} \text{ mol cm}^{-2}$, larger than that on poly- $\text{Co}_4\text{O}_4+\text{RuP}/\text{TiO}_2$ ($6.7 \times 10^{-10} \text{ mol cm}^{-2}$). Therefore, the introduction of Vpa increased the amount of catalyst on the photoanode.

The photocurrent of poly- $\text{Co}_4\text{O}_4+\text{Vpa}/\text{RuP}/\text{TiO}_2$ is shown in Fig. 4, corresponding to the photolysis of water an initial potential 1.2 V (*vs.* NHE). However, under light illumination, as the voltage increases the photocurrent density increases. The current was significantly greater than that of the poly- $\text{Co}_4\text{O}_4+\text{RuP}/\text{TiO}_2$ electrode at the same voltage. This result indicates that the introduction of Vpa may be the main reason for the increase in catalytic current. The photocurrent measurements of PECs were conducted under a 0.4 V bias (*vs.* NHE) upon illumination used a xenon lamp source coupled to a 400 nm long-pass filter (100 mW cm^{-2}). For each of the three photoanodes as show in Fig. 5, a large transient initial photocurrent is obtained and then decreases. The steady state photocurrent density for RuP/TiO_2 (black line) is only $20 \mu\text{A cm}^{-2}$. For poly- $\text{Co}_4\text{O}_4+\text{RuP}/\text{TiO}_2$ (red line) and poly- $\text{Co}_4\text{O}_4+\text{Vpa}/\text{RuP}/\text{TiO}_2$ (blue line), the steady state photocurrent density achieves $45 \mu\text{A cm}^{-2}$ and $80 \mu\text{A cm}^{-2}$, respectively. The poly- $\text{Co}_4\text{O}_4+\text{Vpa}/\text{RuP}/\text{TiO}_2$ photoanode produced a higher photocurrent density compared to poly- $\text{Co}_4\text{O}_4+\text{RuP}/\text{TiO}_2$. When the light is turned on, the giant positive current spike occurs for RuP/TiO_2 and poly- $\text{Co}_4\text{O}_4+\text{RuP}/\text{TiO}_2$ and no spike for poly- $\text{Co}_4\text{O}_4+\text{Vpa}/\text{RuP}/\text{TiO}_2$ (Fig. 5). When

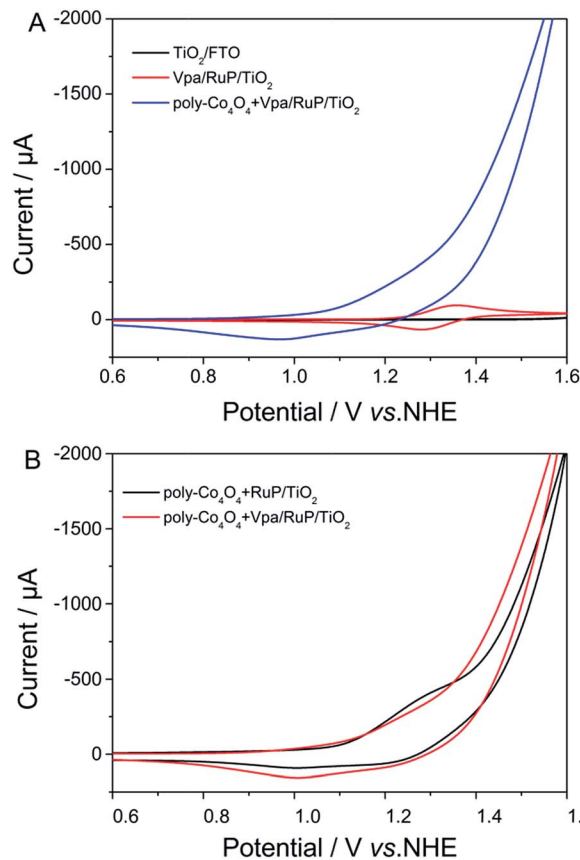


Fig. 3 CV curves of poly- $\text{Co}_4\text{O}_4+\text{Vpa}/\text{RuP}/\text{TiO}_2$ (red line) and $\text{Vpa}/\text{RuP}/\text{TiO}_2$ (black line) (A); poly- $\text{Co}_4\text{O}_4+\text{RuP}/\text{TiO}_2$ (red line) and poly- $\text{Co}_4\text{O}_4+\text{Vpa}/\text{RuP}/\text{TiO}_2$ (black line) (B).

the light was turned off, the RuP/TiO_2 and poly- $\text{Co}_4\text{O}_4+\text{RuP}/\text{TiO}_2$ have apparent reversed current, but the poly- $\text{Co}_4\text{O}_4+\text{Vpa}/\text{RuP}/\text{TiO}_2$ does not have. This result indicates that there was an accumulation of charge for RuP/TiO_2 and poly- $\text{Co}_4\text{O}_4+\text{RuP}/\text{TiO}_2$. A possible explanation is that the Vpa in poly- $\text{Co}_4\text{O}_4+\text{Vpa}/\text{RuP}/\text{TiO}_2$ improve the electronic transport between the

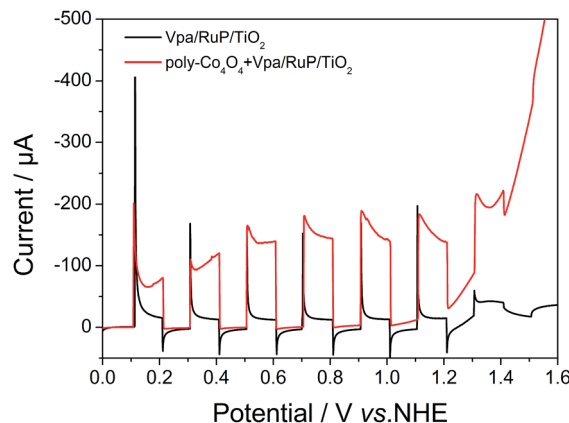


Fig. 4 LSV of poly- $\text{Co}_4\text{O}_4+\text{Vpa}/\text{RuP}/\text{TiO}_2$ (red line) and $\text{Vpa}/\text{RuP}/\text{TiO}_2$ (black line) in Na_2SO_4 solution under illumination with a xenon lamp source coupled to a 400 nm long-pass filter (100 mW cm^{-2}).



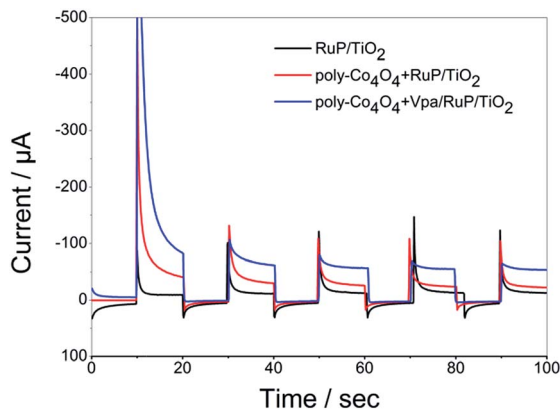


Fig. 5 Photocurrent densities of the light control photocurrent measurements with a 0.4 V (vs. NHE) external bias for poly-Co₄O₄+Vpa/RuP/TiO₂ (blue line), poly-Co₄O₄+RuP/TiO₂ (red line) and RuP/TiO₂ (black line).

photosensitizer and the catalyst, which is another reason for a higher PEC performance for poly-Co₄O₄+Vpa/RuP/TiO₂.

As is shown in Fig. 6, after 500 s light illumination, the photocurrent density remains as high as 70 $\mu\text{A cm}^{-2}$ for poly-Co₄O₄+Vpa/RuP/TiO₂. Compare with other molecular photoanodes previously reported, the poly-Co₄O₄+Vpa/RuP/TiO₂ photoanode showed good stability. On the surface of the photoanode a lot of bubbles can be observed, indicating that oxygen was generated, which can also cause a decrease of the photocurrent. In order to verify the current was produced by the electrolysis of water, we measured the faradaic efficiency of the photoanode using a previously described generator/collector electrode technique.³² A faradaic efficiency of ca. 76% for poly-Co₄O₄+Vpa/RuP/TiO₂ was obtained.

H/D kinetic isotope effect (KIE) measurements

H/D kinetic isotope effect (KIE) measurements were employed by comparing the current densities in H₂O and D₂O. The KIE defines an index of kinetic information regarding water

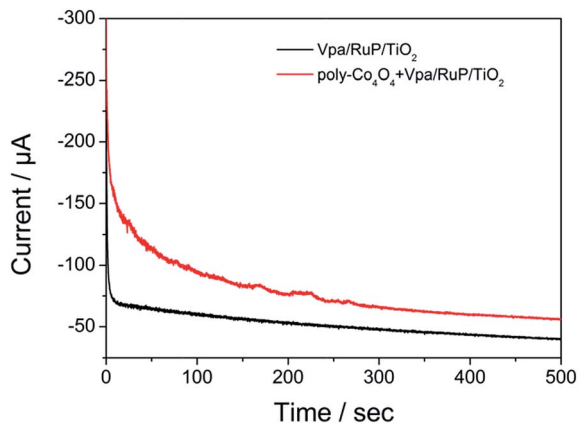


Fig. 6 Amperometric $i-t$ curve with a 0.4 V (vs. NHE) external bias for poly-Co₄O₄+Vpa/RuP/TiO₂ (red line) and Vpa/RuP/TiO₂ (black line) under illumination.

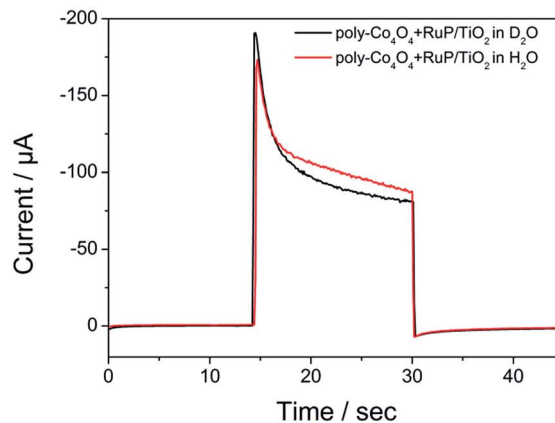
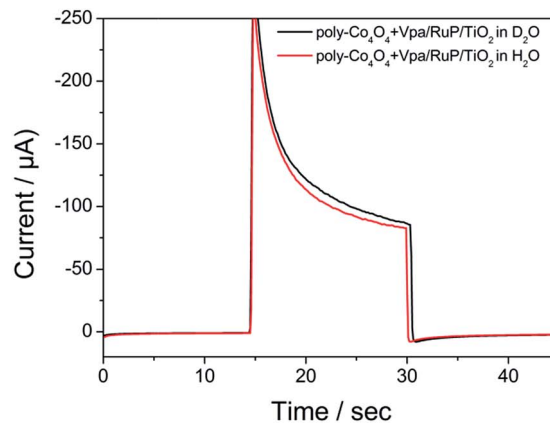


Fig. 7 Photocurrent densities of the light control photocurrent measurements at an applied potential of 0.4 V (vs. NHE) for a poly-Co₄O₄+Vpa/RuP/TiO₂ and poly-Co₄O₄+RuP/TiO₂ in a 0.1 M Na₂SO₄·H₂O (red line) and D₂O (black line) solution.

oxidation reactions and helps chemists interpret the rate-determining step (RDS) of the catalytic processes.^{32–35} From the KIE results, the identical isotope effects were obtained for both poly-Co₄O₄+Vpa/RuP/TiO₂ and poly-Co₄O₄+RuP/TiO₂. In the electrocatalytic process, the current of the electrodes (Fig. S7†) showed significant difference between H₂O and D₂O solutions at 1.70 V (vs. NHE), which means that the RDS for both of the electrodes is the water oxidation step. In the photocatalytic process, a secondary isotope effect ($\text{KIE}_{\text{H/D}} = 0.7\text{--}1.5$) was observed (Fig. 7). A reasonable explanation of the phenomenon is that the electron transport between the photosensitizer and the catalyst is the RDS.

Experimental

Materials

All reagents and solvents were purchased from Aladdin chemical company. Fluoride-doped tin oxide (FTO)-coated glass (thickness ~ 2.2 mm, transmittance $> 90\%$, resistance ~ 8 m Ω cm⁻²) was purchased from Zhuhai kaiwei company, and was cut into 10 mm \times 20 mm strips and used as the substrate for TiO₂ nanoparticle films. All solvents were dried using standard methods. Synthetic reactions were carried out under N₂ or Ar atmosphere using standard Schlenk techniques.



Instruments

^1H NMR was performed on a Bruker AVIII 600 NMR. The mass spectrum was determined on an Agilent UHD 6540 Accurate-Mass Q-TOF MS instrument. The morphology of the modified electrode was measured using a scanning electron microscopy (Hitachi SU8000, Japan). The ultraviolet absorption spectrum of the modified electrodes was determined using the UV-vis spectrophotometer Perkin-Elmer Lambda 35.

Synthesis

$[\text{Ru}(\text{bpy})_2(4,4'-(\text{PO}_3\text{H}_2)_2\text{bpy}_2)]\text{Cl}_2$. This complex was synthesised according to the method reported.²⁹

$\text{Co}_4\text{O}_4(\text{CH}_3\text{CO}_2)_4(\text{vinylpy})_4$ ($\text{py} = \text{pyridine}$) (Co_4O_4). Synthesis of complex Co_4O_4 is according to the procedure reported previously.³⁰ A solution of sodium acetate (1.64 g, 20 mmol) and cobalt nitrate hexahydrate $[\text{Co}(\text{NO}_3)_2 \cdot 6\text{H}_2\text{O}]$ (2.9 g, 10 mmol) in 30 mL methanol was heated at reflux, vinyl pyridine (0.8 mL, 10 mmol) was added during reflux and the reaction mixture was slowly added to 0.5 mL hydrogen peroxide aqueous solution (30%, 50 mmol) dropwise then heated under reflux for 4 h, the methanol was removed by evaporation under reduced pressure. After extraction of the resulting aqueous solution with dichloromethane third and dried over anhydrous sodium sulfate. The dark green crude product solid product was dissolved in a minimum amount of $\text{CH}_2\text{Cl}_2/\text{CH}_3\text{OH} = 10 : 1$ (v/v) and loaded on a silica gel column, was used to attain a pure product (65% yield). $^1\text{H-NMR}$ (600 MHz, CDCl_3): δ 8.52 (d, $J = 6.0$ Hz, 8H), 6.98 (t, $J = 6.0$ Hz, 8H), 6.55–6.51 (m, 4H), 5.91 (d, $J = 18.0$ Hz, 4H), 5.48 (d, $J = 12.0$ Hz, 4H). HR-MS: $m/z = 957.0299$ $[\text{M} + \text{H}]^+$ (calcd: 956.9971) (as Fig. S1†).

Preparation of the photoanodes

TiO_2 was prepared according to the method described.⁷ TiO_2 -sintered FTO electrode TiO_2 film with a 12 μm thickness was made using a knife coating method with ca. 18 nm TiO_2 paste, which was then dried at 120 $^\circ\text{C}$ for 30 min in an oven and annealed at 500 $^\circ\text{C}$ for 30 min, cooled to room temperature to form TiO_2/FTO . The active areas of the photoelectrodes were 1 cm^2 .

RuP/TiO₂. The TiO_2 electrode was sensitised in a solution of 6 mg RuP in 20 mL ethanol for 12 h to obtain RuP@ TiO_2 electrode. It was then washed with ethanol and water several times.

Vpa/RuP/TiO₂. Dry RuP/ TiO_2 anode was then soaked in a methanol solution of 5 mM vinyl phosphate for another 2 h, washed with methanol and water several times and dried in dark at room temperature, then air dried.

Co₄O₄+RuP/TiO₂. Complex Co_4O_4 was polymerised on RuP/ TiO_2 films by electrolysis of a complex Co_4O_4 solution (1 mM $\text{Co}_4\text{O}_4/0.1$ M tetrabutylammonium hexafluorophosphate (TBAPF_6) in anhydrous acetonitrile) at -2.1 V (vs. NHE) for 400 s. The electropolymerisation was carried out in a three-electrode cell under argon atmosphere and the solutions were degassed using argon for at least 10 min prior to reductive electrolysis. The prepared electrode was then washed with acetonitrile several times and dried in dark at room temperature.

Co₄O₄+Vpa/RuP/TiO₂. Complex Co_4O_4 was polymerised on Vpa/RuP/ TiO_2 films using the similar method for the preparation of $\text{Co}_4\text{O}_4+\text{RuP}/\text{TiO}_2$.

Electrochemical and photoelectrochemical measurements

All electrochemical measurements were conducted on CHI Instruments 760E electrochemical potentiostat in a PEC three-electrode cell. A Pt-wire was used as a counter electrode and an aqueous Ag/AgCl (in saturated KNO_3) electrode was used as the reference electrode. The electrolyte solution was a Na_2SO_4 solution (0.1 M) at pH 7.0. A 300 W Xe lamp was used as the light source equipped with a 400 nm long-pass filter (100 mW cm^{-2}).

O₂ measurements

Measurement of evolved O_2 utilized a previously described generator/collector electrode technique four-electrode system the.³¹ A four electrode setup was applied including a Pt counter electrode, saturated Ag/AgCl reference electrode, and two FTO based working electrodes. One FTO (generator) electrode was prepared utilising a poly- $\text{Co}_4\text{O}_4+\text{Vpa}/\text{RuP}/\text{TiO}_2$ photoanode as described in this study; the other FTO (collector) electrode was a clean FTO electrode which was unmodified. The generator/collector electrodes were placed with the conductive sides facing and a thin 0.7 mm thick paperboard placed on both lateral edges between the electrodes. The gap between the two FTO electrodes was filled with 1 M Na_2SO_4 solution at pH 7.0 using capillary action when the cell was placed in solution.

In this experiment, the generator electrode was applied a voltage of 0.4 V (vs. NHE) with illumination from 0 to 300 s and without illumination from 300 to 700 s. The parallel-charge controlled experiments were performed at different collection potentials to differentiate the O_2 reduction and oxidized catalyst/mediator. The optimal of one bias regime was adequately negative potential to reduce the oxidized catalyst/mediator and evolved O_2 (Q_{CH}). Q_{CH} was measured at -1.05 V (vs. NHE). The collector was poised at a more positive potential before the onset of O_2 reduction at -0.55 V (vs. NHE) to measure the current reduction of the oxidized catalyst/mediator (Q_{CL}).

Determination of the faradaic efficiency (η_{O_2}). η_{O_2} was calculated by the total charge attribute to O_2 reduction ($Q_{\text{CH}} - Q_{\text{CL}}$), divided by the total charge passed at the generator electrode (Q_{GH}). The faradaic efficiency was corrected for the collection efficiency of this setup (70%) that was determined experimentally.

Conclusions

In conclusion, two types of photoanodes that consist of a molecular catalyst and a photosensitiser have been successfully assembled through the electrochemically polymerisation of a vinyl-modified cobalt cubane catalyst. $\text{Co}_4\text{O}_4(\text{O}_2\text{CME})_4(4\text{-vinylpy})_4$ was polymerised on a RuP-sensitised TiO_2 and on TiO_2 surface codecorated with Vpa and RuP, and a poly- $\text{Co}_4\text{O}_4/\text{RuP}/\text{TiO}_2$ were obtained. Using these photoanodes in a three-electrode system, the functional device assembled containing poly- $\text{Co}_4\text{O}_4+\text{Vpa}/\text{RuP}/\text{TiO}_2$ demonstrated better performance in light driven water oxidation than the device containing poly-



Co₄O₄/RuP/TiO₂. During long-term light control measurements, a photocurrent density of ~100 μA cm⁻² was achieved in Na₂SO₄ solution at pH 7.0 under a 0.4 V external environment, with a faradaic efficiency of 76% for oxygen production. The KIE studies suggested that electron transport between the photosensitiser and the catalyst was the RDS in the PEC reaction. The PEC measurements demonstrate that the electropolymerised techniques explored in this study is possibly a viable means of preparing photocatalytically photoanodes. The Vpa chain in poly-Co₄O₄+Vpa/RuP/TiO₂ plays an important role in the immobilisation of the catalysis and enhancement of electron transport between the photosensitiser and the catalyst. Further work is being undertaken to explore superior linkage between the catalyst and photosensitiser with the aim of improving the stability of this molecular device.

Acknowledgements

This work was supported by the National Natural Science Foundation of China (21401092, 21671089, 21271095, 21303187) the Doctor Subject Foundation of the Ministry of Education of China (20132101110001), the Shenyang Natural Science Foundation of China (F16-103-4-00), Scientific Research Fund of Liaoning Provincial Education Department (L2014005, LT2015012, and LJQ2014003), the State Key Laboratory of Fine Chemicals (KF 1404).

Notes and references

- 1 A. Fujishima and K. Honda, *Nature*, 1972, **238**, 37–38.
- 2 M. Grätzel, *Nature*, 2001, **414**, 338–344.
- 3 Z. Yu, F. Li and L. Sun, *Energy Environ. Sci.*, 2015, **8**, 760–775.
- 4 D. Kang, T. W. Kim, S. R. Kubota, A. C. Cardiel and H. G. Cha, *Chem. Rev.*, 2015, **115**, 12839–12887.
- 5 Z. S. Li, W. J. Luo, M. L. Zhang, J. Y. Feng and Z. G. Zou, *Energy Environ. Sci.*, 2013, **6**, 347–370.
- 6 T. Hisatomi, J. Kubota and K. Domen, *Chem. Soc. Rev.*, 2014, **43**, 7520–7535.
- 7 Y. Gao, X. Ding, J. Liu, L. Wang, Z. Lu, L. Li and L. Sun, *J. Am. Chem. Soc.*, 2013, **135**, 4219–4222.
- 8 K. Hanson, D. A. Torelli, A. K. Vannucci, M. K. Brennaman, H. Luo, L. Alibabaei, W. Song, D. L. Ashford, M. R. Norris, C. R. K. Glasson, J. J. Concepcion and T. J. Meyer, *Angew. Chem., Int. Ed.*, 2012, **51**, 12782–12785.
- 9 M. D. Kärkäs, O. Verho, E. V. Johnston and B. Åkermark, *Chem. Rev.*, 2014, **114**, 11863–12001.
- 10 Y. Jiang, F. Li, F. Huang, B. B. Zhang and L. C. Sun, *Chin. J. Catal.*, 2013, **34**, 1489–1495.
- 11 L. L. Duan, A. Fischer, Y. H. Xu and L. C. Sun, *J. Am. Chem. Soc.*, 2009, **131**, 10397–10399.
- 12 Y. Jiang, F. Li, B. B. Zhang, X. N. Li, X. H. Wang, F. Huang and L. C. Sun, *Angew. Chem., Int. Ed.*, 2013, **52**, 3398–3410.
- 13 L. L. Duan, F. Bozoglian, S. Mandal, B. Stewart, T. Privalov, A. Llobet and L. C. Sun, *Nat. Chem.*, 2012, **4**, 418–423.
- 14 J. F. Hull, D. Balcells, J. D. Blakemore, C. D. Incarvito, O. Eisenstein, G. W. Brudvig and R. H. Crabtree, *J. Am. Chem. Soc.*, 2009, **131**, 8730–8731.
- 15 J. M. Thomsen, D. L. Huang, R. H. Crabtree and G. W. Brudvig, *Dalton Trans.*, 2015, **44**, 12452–12472.
- 16 N. S. McCool, D. M. Robinson, J. E. Sheats and G. C. Dismukes, *J. Am. Chem. Soc.*, 2011, **133**, 11446–11449.
- 17 G. La Ganga, F. Puntoriero, S. Campagna, I. Bazzan, S. Berardi, M. Bonchio, A. Sartorel, M. Natali and F. Scandola, *Faraday Discuss.*, 2012, **155**, 177–190.
- 18 S. Berardi, G. La Ganga, M. Natali, I. Bazzan, F. Puntoriero, A. Sartorel, F. Scandola, S. Campagna and M. J. Bonchio, *J. Am. Chem. Soc.*, 2012, **134**, 11104–11107.
- 19 G. F. Moore, J. D. Blakemore, R. L. Milot, J. F. Hull, H. Song, L. Cai, C. A. Schmuttenmaer, R. H. Crabtree and G. W. Brudvig, *Energy Environ. Sci.*, 2011, **4**, 2389–2392.
- 20 W. J. Youngblood, S. H. A. Lee, Y. Kobayashi, E. A. Hernandez-Pagan, P. G. Hoertz, T. A. Moore, A. L. Moore, D. Gust and T. E. Mallouk, *J. Am. Chem. Soc.*, 2009, **131**, 926–927.
- 21 Y. Zhao, J. R. Swierk, J. D. Megiatto, B. Sherman, W. J. Youngblood, D. Qin, D. M. Lentz, A. L. Moore, T. A. Moore, D. Gust and T. E. Mallouk, *Proc. Natl. Acad. Sci. U. S. A.*, 2012, **109**, 15612–15616.
- 22 L. Alibabaei, M. K. Brennaman, M. R. Norris, B. Kalanyan, W. Song, M. D. Losego, J. J. Concepcion, R. A. Binstead, G. N. Parsons and T. J. Meyer, *Proc. Natl. Acad. Sci. U. S. A.*, 2013, **110**, 20008–20013.
- 23 H. Li, F. Li, Y. Wang, L. C. Bai, F. S. Yu and L. C. Sun, *ChemPlusChem*, 2016, **81**, 1056–1059.
- 24 X. Ding, Y. Gao, L. Zhang, Z. Yu, J. Liu and L. C. Sun, *ACS Catal.*, 2014, **4**, 2347–2350.
- 25 B. B. Zhang, F. Li, F. S. Yu, Xi. H. Wang, X. Zhou, H. Li, Y. Jiang and L. C. Sun, *ACS Catal.*, 2014, **4**, 804–809.
- 26 D. L. Ashford, A. M. Lapidés, A. K. Vannucci, K. Hanson, D. A. Torelli, D. P. Harrison, J. L. Templeton and T. J. Meyer, *J. Am. Chem. Soc.*, 2014, **136**, 6578–6581.
- 27 D. L. Ashford, B. D. Sherman, R. A. Binstead, Jo. L. Templeton and T. J. Meyer, *Angew. Chem., Int. Ed.*, 2015, **54**, 4778–4781.
- 28 F. S. Li, K. Fan, L. Wang, Q. Daniel, L. L. Duan and L. C. Sun, *ACS Catal.*, 2015, **5**, 3786–3790.
- 29 S. Caramori, V. Cristino, R. Argazzi, L. Meda and C. A. Bignozzi, *Inorg. Chem.*, 2010, **49**, 3320–3328.
- 30 X. Li and P. E. M. Siegbahn, *J. Am. Chem. Soc.*, 2013, **135**, 13804–13813.
- 31 D. L. Ashford, B. D. Sherman, R. A. Binstead, J. L. Templeton and T. J. Meyer, *Angew. Chem., Int. Ed.*, 2015, **54**, 4778–4781.
- 32 D. Moonshiram, V. Purohit, J. Concepcion, T. Meyer and Y. Pushkar, *Materials*, 2013, **6**, 392–409.
- 33 H. Yamada, W. F. Siems, T. Koike and J. K. Hurst, *J. Am. Chem. Soc.*, 2004, **126**, 9786–9795.
- 34 F. Liu, J. J. Concepcion, J. W. Jurss, T. Cardolaccia, J. L. Templeton and T. J. Meyer, *Inorg. Chem.*, 2008, **47**, 1727–1752.
- 35 Z. Chen, J. J. Concepcion, X. Hu, W. Yang, P. G. Hoertz and T. J. Meyer, *Proc. Natl. Acad. Sci. U. S. A.*, 2010, **107**, 7225–7229.

